

Intestinal IL-1 β Plays a Role in Protecting against SARS-CoV-2 Infection

Jöran Lücke,^{*,†,‡,1} Fabian Heinrich,^{§,¶,1} Jakob Malsy,^{||,‡,***} Nicholas Meins,^{*,†} Josa Schnell,^{*,†} Marius Böttcher,^{*,†,||} Mikolaj Nawrocki,^{*,†,||} Tao Zhang,^{*,†} Franziska Bertram,^{*,†,||} Morsal Sabihi,^{*,†} Jan Kempinski,^{*,†,||,††} Tom Blankenburg,^{*,†,‡} Anna Duprée,[‡] Matthias Reeh,[‡] Stefan Wolter,[‡] Oliver Mann,[‡] Jakob R. Izbicki,[‡] Ansgar W. Lohse,^{†,||} Nicola Gagliani,^{*,†,‡} Marc Lütgehetmann,[¶] Madeleine J. Bunders,^{#,‡,‡} Marcus Altfeld,[#] Guido Sauter,^{§§} Anastasios D. Giannou,^{*,†,‡} Susanne Krasemann,^{¶¶} Benjamin Ondruschka,^{§,2} and Samuel Huber^{*,†,||,2}

The intestine is constantly balancing the maintenance of a homeostatic microbiome and the protection of the host against pathogens such as viruses. Many cytokines mediate protective inflammatory responses in the intestine, among them IL-1 β . IL-1 β is a proinflammatory cytokine typically activated upon specific danger signals sensed by the inflammasome. SARS-CoV-2 is capable of infecting multiple organs, including the intestinal tract. Severe cases of COVID-19 were shown to be associated with a dysregulated immune response, and blocking of proinflammatory pathways was demonstrated to improve patient survival. Indeed, anakinra, an Ab against the receptor of IL-1 β , has recently been approved to treat patients with severe COVID-19. However, the role of IL-1 β during intestinal SARS-CoV-2 infection has not yet been investigated. Here, we analyzed postmortem intestinal and blood samples from patients who died of COVID-19. We demonstrated that high levels of intestinal IL-1 β were associated with longer survival time and lower intestinal SARS-CoV-2 RNA loads. Concurrently, type I IFN expression positively correlated with IL-1 β levels in the intestine. Using human intestinal organoids, we showed that autocrine IL-1 β sustains RNA expression of IFN type I by the intestinal epithelial layer. These results outline a previously unrecognized key role of intestinal IL-1 β during SARS-CoV-2 infection. *The Journal of Immunology*, 2023, 211: 1052–1061.

The intestine is colonized by billions of different microbes (1, 2) that aid the host in defending against foreign pathogens (3) or digesting nutrients (4). Thus, the intestinal immune system requires highly flexible but tight regulation to balance tolerance and inflammation (5). This is achieved by a sophisticated interplay between intestinal immune cells, their secreted chemokines or cytokines, and the microbiome (6). One

of these intestinal cytokines with grand implications in homeostasis and disease is IL-1 β (7).

IL-1 β is a proinflammatory cytokine belonging to the IL-1 family (8). It is mainly produced by tissue macrophages (9) but can also be secreted by various other cells, such as neutrophils (10) or epithelial cells (11, 12). IL-1 β then binds to the IL-1 receptor (IL-1R) (13), a receptor expressed on a variety of different cell subsets (14).

*Section of Molecular Immunology and Gastroenterology, I Department of Medicine, University Medical Center Hamburg-Eppendorf, Hamburg, Germany; †Hamburg Center for Translational Immunology, University Medical Center Hamburg-Eppendorf, Hamburg, Germany; ‡Department of General, Visceral and Thoracic Surgery, University Medical Center Hamburg-Eppendorf, Hamburg, Germany; §Institute of Legal Medicine, University Medical Center Hamburg-Eppendorf, Hamburg, Germany; ¶Institute of Medical Microbiology, Virology, and Hygiene, University Medical Center Hamburg-Eppendorf, Hamburg, Germany; ||I Department of Medicine, University Medical Center Hamburg-Eppendorf, Hamburg, Germany; #Leibniz Institute of Virology, Hamburg, Germany; **German Center for Infection Research, Hamburg-Lubeck-Borstel-Riems, Germany; ††Mildred Scheel Cancer Career Center HaTriCS4, University Medical Center Hamburg-Eppendorf, Hamburg, Germany; ‡‡III Department of Medicine, University Medical Center Hamburg-Eppendorf, Hamburg, Germany; §§Institute of Pathology, University Medical Center Hamburg-Eppendorf, Hamburg, Germany; and ¶¶Institute for Neuropathology, University Medical Center Hamburg-Eppendorf, Hamburg, Germany

¹J.L. and F.H. share first authorship and contributed equally to this work.

²B.O. and S.H. share last authorship and contributed equally to this work.

ORCID: 0000-0002-6081-479X (J.L.); 0000-0001-6866-0257 (J.M.); 0000-0003-3685-9389 (J.S.); 0000-0002-8579-7236 (M.N.); 0000-0001-9331-8832 (T.Z.); 0000-0001-9840-0931 (M.S.); 0009-0001-1952-1207 (T.B.); 0000-0003-3323-122X (A.D.); 0000-0002-8823-3129 (A.W.L.); 0000-0002-9468-7944 (M.L.); 0000-0001-8795-818X (S.K.); 0000-0001-9325-8227 (S.H.).

Received for publication November 15, 2022. Accepted for publication July 11, 2023.

This work was supported in part by the Deutsche Forschungsgemeinschaft (Grant SFB841 to S.H., N.G., and A.W.L. and Grant SFB1328 to S.H. and N.G.), Ernst Jung-Stiftung Hamburg (to S.H.), Stiftung Experimentelle Biomedizin (to S.H.), the NATON consortium as part of the Netzwerk Universitätsmedizin funded by the Federal Ministry of Education and Research of Germany (grant 01KX2121 to B.O., F.H., and S.K.), EFRE 2014-2020

REACT-EU (to M.J.B.), and the Deutsche Krebshilfe (70114853 to A.D.G.). S.H. has an endowed Heisenberg Professorship awarded by the Deutsche Forschungsgemeinschaft.

J.L. and F.H. conceived and designed all experiments, analyzed data, and performed experiments; J.L. wrote the manuscript; J.M. designed and carried out all in vitro experiments regarding organoids; N.M. and J.S. performed RNA extraction and quantitative PCR assays; M.B. provided the out-of-surgery human samples, provided critical intellectual input, and edited the paper; M.N., T.Z., F.B., M.S., and J.K. provided critical intellectual input and edited the paper; T.B. performed RNA extraction and quantitative PCR assays; A.D., M.R., S.W., O.M., J.R.I., A.W.L., and N.G. provided critical intellectual input and edited the paper; M.L. performed measurements of SARS-CoV-2 levels, provided critical intellectual input, and edited the paper; M.J.B. and M.A. designed organoid experiments, provided critical intellectual input, and edited the paper; G.S. provided the out-of-surgery human samples, provided critical intellectual input, and edited the paper; A.D.G. provided critical intellectual input and edited the paper; S.K. designed and performed experiments regarding immunofluorescence and immunohistochemistry, provided critical intellectual input, and edited the paper; B. O. and S.H. conceived the idea for the study and supervised the study. All authors reviewed and agreed with the submitted manuscript.

Address correspondence and reprint requests to Prof. Samuel Huber, University Medical Center Hamburg-Eppendorf, Martinistraße 52, 20246, Hamburg, Germany. E-mail address: shuber@uke.de

The online version of this article contains supplemental material.

Abbreviations used in this article: BMI, body mass index; IL-1R, IL-1 receptor; PMI, postmortem interval; RT-qPCR, RT-quantitative PCR; S-protein, Spike protein.

This article is distributed under The American Association of Immunologists, Inc., [Reuse Terms and Conditions for Author Choice articles](#).

Copyright © 2023 by The American Association of Immunologists, Inc. 0022-1767/23/\$37.50

Although pivotal in inducing a robust immune response against pathogens (15), a more pathogenic role of IL-1 β has been discovered in the last decade. It is mainly attributed to its capacity to induce or enhance type 3–centered immune responses (16). In this setting, the production of cytokines such as IL-17A, IL-17F, or IL-22 by cells such as Th cells (16) or $\gamma\delta$ T cells plays a key role (17). In this regard, IL-1 β was linked to unfavorable effects in cancer (18), metastasis (19, 20), and inflammatory bowel disease (21, 22).

In line with its proinflammatory functions, many studies found elevated serum levels of IL-1 β in patients during multiple viral diseases such as influenza (23) or chronic hepatitis C (24). Surprisingly, evidence of systemic upregulation of IL-1 β during one of the latest viral infections, namely SARS-CoV-2 infection, is more ambiguous (25–28). However, a robust upregulation of IL-1 β could be detected in bronchial lavage fluid (29, 30) and histological lung sections of individuals with SARS-CoV-2 infection (31, 32).

To infect cells, SARS-CoV-2 binds via its Spike protein (S-protein) to the angiotensin-converting enzyme 2 on the cell surface (33) and triggers the production of proinflammatory components such as IL-6, TNF- α , and also IL-1 β (34). Although it has often been reported that monocytes are the main source of IL-1 β upon SARS-CoV-2 infection (29, 35, 36), some studies also describe IL-1 β production by bronchial epithelial cells (37). Likewise, SARS-CoV-2 infection also leads to increased production of type I IFNs (38–41), such as IFN- α 2 and IFN- β 1, that are essential in mediating an early antiviral response (42).

Although these bronchial epithelial cells are the first targets of SARS-CoV-2 infection (43), the virus can proceed to infect other organs. Using postmortem case collections, the detection of SARS-CoV-2 in the heart (44), the kidneys (45, 46), or the liver (47, 48) was demonstrated already. The gastrointestinal tract is another organ with high expression levels of the angiotensin-converting enzyme 2 entry protein (49). Studies using primary human-derived (50, 51) or bat-derived organoids (51) showed replication of SARS-CoV-2 in vitro. Moreover, in patient cohorts, gastrointestinal symptoms, such as emesis or diarrhea, were shown to be associated with increased survival (52), suggestive of the great importance of the gut during SARS-CoV-2 infections. However, underlying mechanisms and tissue-specific immune responses in the intestine upon SARS-CoV-2 infection remain elusive.

It is now widely accepted that severe COVID-19 is associated with dysregulated immune responses that may ultimately culminate in a cytokine storm (53). For example, high levels of different cytokines, such as IL-6, IL-8, and TNF- α , were associated with impaired survival (25). In line with this, we found that high *TNFA* expression in the liver correlates with a reduced survival time (54). These observations led to a rapid reevaluation of already well-established immune-modifying agents initially developed to target autoimmune diseases such as rheumatoid arthritis or inflammatory bowel disease. To date, many of these agents have proved beneficial in combating severe cases of COVID-19, including therapies directed against the JAK pathway (55) or IL-6 (56). Most recently, anakinra, an Ab targeting IL-1R, was approved against SARS-CoV-2 infection (57). Given the emerging role of the intestine during SARS-CoV-2 infection on the one hand and IL-1 β 's generally protective functions in the intestine on the other, detailed investigations into this interplay are warranted. To begin with, it is unclear if there is a different impact of systemically distributed versus intestine-produced IL-1 β . Furthermore, the sources and functions of IL-1 β in the intestine during SARS-CoV-2 infection are unknown.

In this study, we investigated the influence of systemic and intestinal IL-1 β by analyzing its expression in 45 patients who died of SARS-CoV-2 infection. High levels of *IL1B* mRNA expression in the blood of this cohort were associated with a reduced survival time.

However, elevated expression of this cytokine in the intestine was associated with increased survival time. Moreover, patients with high intestinal *IL1B* expression and detectable SARS-CoV-2 RNA showed a reduced intestinal viral load, whereas high systemic *IL1B* expression did not correlate with the viral load in the blood. An increased intestinal viral load was also an independent risk factor for reduced survival time in our cohort. Furthermore, our investigation shows that macrophages and intestinal epithelial cells might be the source of IL-1 β , which, in turn, sustains the RNA expression of the antiviral cytokine *IFN α 2* in the intestinal epithelial layer upon S-protein stimulation in vitro. In summary, these results point toward a protective role of intestinal IL-1 β during SARS-CoV-2 infection.

Materials and Methods

Autopsies and collection of clinical data

The data and sample acquisition were performed between April 2020 and April 2021. A total of 45 COVID-19 death cases admitted to the Institute of Legal Medicine were included in the study. For an initial assessment of SARS-CoV-2 RNA, RT-quantitative PCR (RT-qPCR) from nasopharyngeal swab samples was performed as part of routine diagnostic tests at the Institute of Microbiology, Virology, and Hygiene. The cause of death was evaluated according to current literature (58). Patients not dying of but with COVID-19 were strictly excluded from the analysis. Corpses exhibiting advanced putrefactive changes were also excluded. All corpses were stored at 4°C upon admission to the Institute of Legal Medicine. Full autopsies were performed at the Institute of Legal Medicine of the University Medical Center Hamburg-Eppendorf, following the German Society of Legal Medicine guidelines, considering recent guidelines on postmortem specimens from deceased individuals with confirmed or suspected COVID-19. Tissue samples were collected as triplicates from the duodenum and blood and were immediately snap-frozen in liquid nitrogen until further use. Sociodemographic and clinical data, such as preexisting medical conditions, specific disease symptoms, and laboratory results upon SARS-CoV-2 diagnosis, were acquired from the patient records from nursing homes, hospitals, or private practices.

RT-qPCR for cytokines

Total RNA from the respective tissues was extracted using the RNeasy Plus Mini Kit (Qiagen, Hilden, Germany) according to the manufacturer's instructions. After the RNA yield was measured and adjusted, the high-capacity cDNA synthesis kit (Applied Biosystems, Waltham, MA) was used for cDNA synthesis. Real-time PCR was carried out using the Kapa Probe Fast qPCR Master Mix (Kapa Biosystems, Wilmington, MA) on the StepOne Plus system (Applied Biosystems). Probes were purchased from Applied Biosystems (Table I). The relative expression was normalized to HPRT and calculated using the $2^{-\Delta\Delta Ct}$ method.

RT-qPCR for SARS-CoV-2

The protocol was carried out as previously reported (47). The tissue samples were ground (Precellys 24; Bertin Instruments, Rockville, MD) in 2-ml tubes filled with ceramic beads (Precellys Lysing Kit) and PBS. A 200- μ l aliquot of

Table I. Probes used in this study for human RNA quantification with RT-qPCR

Gene	Probe name
<i>FOXP3</i>	Hs01058534_m1
<i>HPRT1</i>	Hs02800695_m1
<i>IFNA2</i>	Hs00265051_s1
<i>IFNB1</i>	Hs01077958_s1
<i>IFNG</i>	Hs00989291_m1
<i>IL1B</i>	Hs00174097_m1
<i>IL6</i>	Hs00174131_m1
<i>IL10</i>	Hs00961622_m1
<i>IL17A</i>	Hs00174383_m1
<i>IL17F</i>	Hs00369400_m1
<i>IL22</i>	Hs01574154_m1
<i>IL23</i>	Hs00900828_g1
<i>RORC</i>	Hs01076122_m1
<i>TBX21</i>	Hs00203436_m1
<i>TGFB1</i>	Hs00998133_m1
<i>TNF</i>	Hs01113624_g1

this lysate was used for extraction through MagnaPure96 (Roche, Mannheim, Germany). The primer (5'-ACAGGTACGTAAATAGTTAATAGCmGT-3', 400 nM end concentration; 5' TATTGCAGCAGTACGCACmCA-3', 400 nM end concentration) and probe (5'-Fam- ACACAGCC/ZEN/ATCCT-TACTGCGCTTCG-Iowa Black FQ-3', 100 nM end concentration) used were from Integrated DNA Technologies (Leuven, Belgium). One-step RT-PCR (25- μ l volume) was performed using the LightCycler 480 system (Roche) with a one-step RNA control kit (Roche) as the master mix and 5 μ l eluate. The C_T value for the target SARS-CoV-2 RNA was measured using the second derivative maximum method. Standard RNA reference material (obtained from INSTAND e.V., Düsseldorf, Germany) was used for quantification. Quantitative β -globin PCR was carried out with the respective TaqMan primer set (Thermo Fisher; 401846) and a DNA control kit (Roche). Samples were run on the LightCycler 480 system. SARS-CoV-2 RNA levels in tissues were then normalized to β -globin DNA. A sample with a C_T value >40 was set as a sample with undetectable SARS-CoV-2 RNA.

Immunohistochemical analysis

Gut tissues were fixed in 4% buffered formalin, dehydrated, and embedded in paraffin. Paraffin tissue sections were cut at 3 μ m. After dewaxing and inactivation of endogenous peroxidases (PBS with 3% hydrogen peroxide), Ab-specific Ag retrieval was performed using the Ventana Benchmark XT device (Ventana, Tucson, AZ). Ultimately, slides were incubated with an Ab against IL-1 β (ab9722, dilution 1:500; Abcam, Cambridge, UK) for 1 h. The UltraView Universal DAB Detection Kit (760-500; Roche) was used as a secondary Ab. Counterstaining and bluing were performed with hematoxylin (760-2021; Ventana Roche) and Bluing Reagent (760-2037; Ventana Roche) for 4 min. Subsequently, stained sections were mounted in a mounting medium. One section was evaluated per organ and/or patient.

Immunofluorescence

Tissues were fixed in 4% buffered formalin, dehydrated, and embedded in paraffin. Sections (3 μ m) were mounted on glass slides, first treated in xylene and increasing ethanol solutions, then hydrated and washed in H₂O. Sections were heated in a rice cooker with 10 mM sodium citrate buffer (pH 6) for 1 h, subsequently washed with H₂O, and then incubated in PBS-Triton 0.2%. After washing, sections were incubated for 60 min in a blocking buffer. Samples were stained overnight with Abs against IL-1 β (ab9722, dilution 1:500; Abcam) and IBA1 (234004; dilution 1:500; Synaptic Systems) at 4°C. After washing, secondary Ab staining was carried out for 1.5 h at room temperature. Nuclei were counterstained with DAPI solution. Fluorescence microscopy was carried out using an SP5 confocal microscope (Leica, Heidelberg, Germany).

Isolation, culture, and stimulation of human intestinal organoids

Suspension organoids from human intestinal tissue samples with the apical epithelium facing outward were established as described previously (59). Briefly, epithelial cells were isolated from human intestinal tissue samples and cultured in an expansion medium. Intestinal organoids were passaged at least twice before experiments. After 5 d of growth, Matrigel was removed, and organoids were cultured in a differentiation medium. Experiments were conducted after 5 more days. Organoids were stimulated for 10 h for ELISA and 24 h for qPCR assays with flagellin 100 ng/ml (catalog number tlr-epstfla; InvivoGen, San Diego, CA), LPS 100 ng/ml (catalog number L3024; Sigma-Aldrich, Burlington, MA), SARS-CoV-2 S-protein 1 μ g/ml (catalog number 130-127-951; Miltenyi Biotec, Bergisch Gladbach, Germany), and/or 10 μ g/ml α -IL-1 β (catalog number 511601, clone H1b-27; BioLegend, San Diego, CA). During stimulation, A8031 and N-acetyl cysteine were removed from the medium.

ELISA

The ELISAs for detection of IL-1 β (catalog number DLB50; R&D Systems, Minneapolis, MN), IFN- α 2 (catalog number HSIFNA2; R&D Systems), and IFN- β 1 (catalog number QK410; R&D Systems) were carried out according to the manufacturer's instructions (R&D Systems).

Isolation, culture, and stimulation of human macrophages

Blood was drawn from healthy volunteers into EDTA-coated tubes, and leukocytes were subsequently isolated using a Ficoll gradient. Monocytes and macrophages were isolated using MACS with anti-CD14 human magnetic beads (catalog number 130-050-201; Miltenyi Biotec). Cells were seeded into 24-well plates in a concentration of 0.5 million cells per well in cell culture medium (containing RPMI 1640, 10% FBS, and 1% penicillin/streptomycin), supplemented with M-CSF (50 ng/ml). The medium was changed at day 3 and day 6. Experiments were conducted 6 d after initial isolation. Macrophages were stimulated for 24 h with LPS 100 ng/ml (catalog number L3024; Sigma-Aldrich), SARS-CoV-2 S-protein 1 μ g/ml (catalog number 130-127-951; Miltenyi Biotec), and/or 1 μ g/ml α -IL-1 β (catalog number 511601, clone H1b-27; BioLegend).

Statistics

Data are presented as absolute and relative frequencies for categorical variables and as the median and interquartile range for continuous variables. As appropriate, the comparison of categorical variables was made using Fisher's exact test or the χ^2 test. Continuous variables were compared using the Mann-Whitney *U* test. Correlation coefficients were estimated using a pairwise correlation between variables, with pairwise deletion of observations in case of missing values by default. Bonferroni-adjusted significance levels are given if required. Survival function estimates were calculated using the Kaplan-Meier method and were compared using the log-rank test. To investigate the predictive value of intestinal *IL1B* levels, we performed a median split of *IL1B* expression in the intestine and the blood, respectively. A *p* value <0.05 , adjusted when appropriate, was considered statistically significant. The statistical analysis was done using STATA/MP version 17.0 (StataCorp, College Station, TX). GraphPad Prism software version 9.1.1 (GraphPad Software, La Jolla, CA) was used for data illustration. Graphical illustrations were created using BioRender.com.

Study approval

For autopsy studies, the informed consent of relatives or legal representatives was obtained. This study was approved by the ethics committee of the Hamburg Chamber of Physicians (reference numbers PV7311 and 2020-10353-BO-ff) and conducted according to the guidelines of the Declaration of Helsinki.

The collection of human intestinal tissues was also approved by the ethics committee of the Hamburg Chamber of Physicians (reference number PV5251). Intestinal tissue samples were only collected upon receiving the patient's informed consent.

Results

High levels of IL1B in the intestine are associated with an increased survival time

To investigate the role of the tissue-specific immune response of the gut during SARS-CoV-2 infection, we analyzed the RNA expression of 16 genes of matched autopsy tissue samples from the duodenum and whole blood of 45 individuals who died of COVID-19 (Fig. 1A and Table I). The median patient age was 79 y (interquartile range, 71–85), with 16 (36%) of 45 being female. Further baseline clinical characteristics are illustrated in Table II. To investigate the association of intestinal IL-1 β on survival time, we divided the cohort according to the median of relative *IL1B* expression in the intestine and the blood, respectively. As a housekeeping gene, *HPRT1* expression was assessed in all tissue samples. Comparison of the *IL1B*^{high} and *IL1B*^{low} groups did not show significant differences regarding sex, body mass index (BMI), age, postmortem interval (PMI), and general hospitalization (Fig. 1B).

High expression of *IL1B* in the blood was significantly associated with a reduced survival period, defined as the time between the first known positive SARS-CoV-2 qPCR test and death (*p* = 0.01) (Fig. 1C). Surprisingly, the observed association between survival and *IL1B* levels in the gastrointestinal tract was inverse. In this tissue, high *IL1B* expression was significantly associated with a prolonged survival period (*p* = 0.04) (Fig. 1D). However, no linear correlation was found between intestinal and whole blood *IL1B* (R^2 = 0.002; *p* = 0.75) (Fig. 1E), suggesting that *IL1B* expression in these compartments is regulated independently. Next, with opposing effects of *IL1B* in mind, we asked whether levels of *IL1B* might also differ between compartments. Indeed, *IL1B* was expressed at a significantly higher level in the blood than in the small intestine (*p* < 0.0001) (Fig. 1F), potentially explaining the beneficial effect of IL-1R blockade in some patients (57). Taken together, high levels of *IL1B* in the intestine are associated with an increased survival time, whereas the opposite is seen in the blood.

Systemic IL1B is not associated with the systemic viral load but correlates with a decreased survival time and an enhanced TGF- β (TGFB) response

We next hypothesized that levels of IL-1 β in the blood might influence the systemic load of SARS-CoV-2 mRNA. However, no difference was found between *IL1B*^{high} and *IL1B*^{low} groups in the blood when comparing the average C_T levels of associated SARS-CoV-2

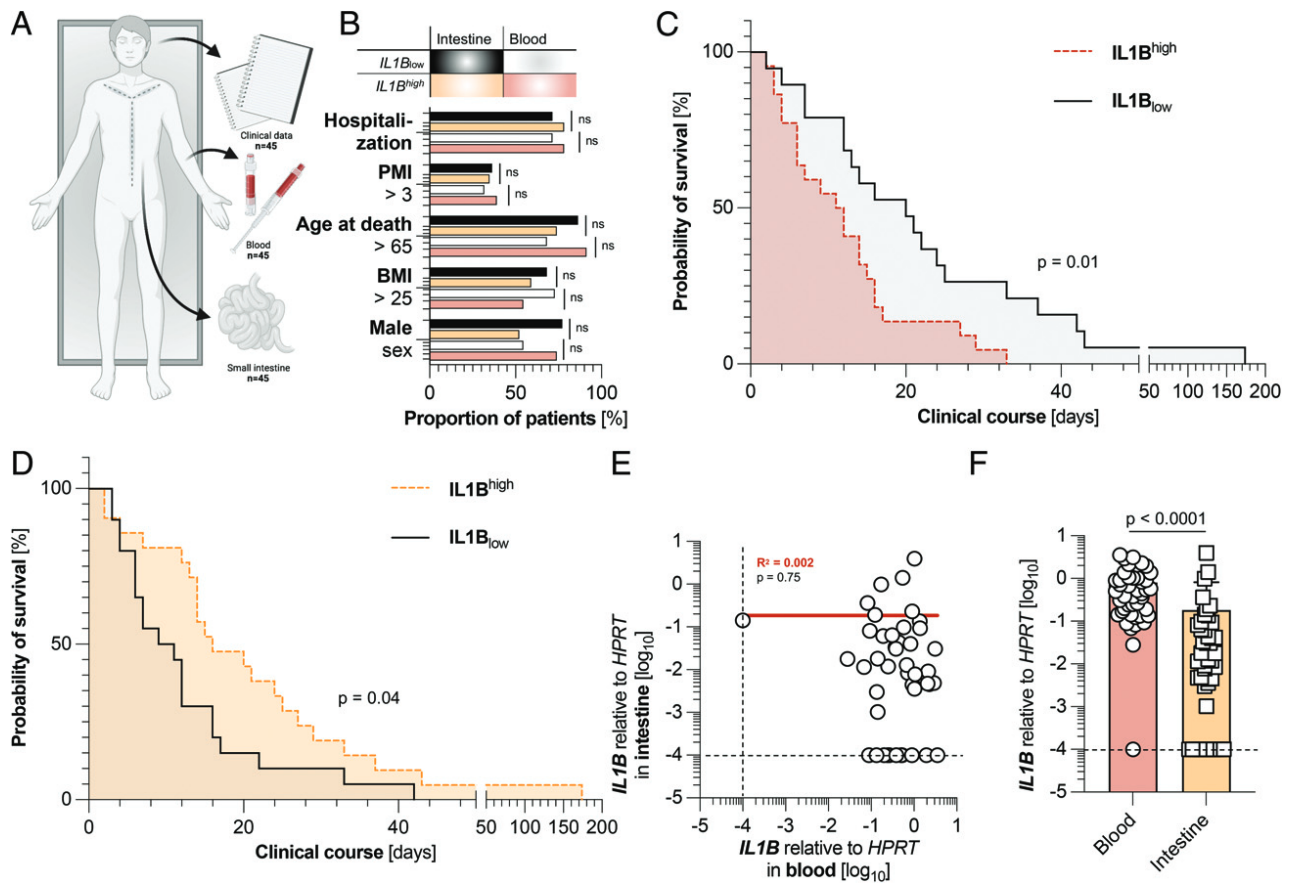


FIGURE 1. Expression levels of *IL1B* in the blood and the intestine are associated with inverse survival times. (A) Schematic picture of the data collection process in which clinical data and tissue samples of blood and duodenum were collected from 45 individuals who died of COVID-19. (B) Cohort characteristics of patients with low (below the median) intestinal expression of *IL1B* ($n = 22$, black) or high (above the median) intestinal expression of *IL1B* ($n = 23$, yellow), as well as low (below the median) expression of *IL1B* in the blood ($n = 22$, white) and high (above the median) expression of *IL1B* in the blood ($n = 22$, red). One blood sample had to be excluded due to undetectable *HPRT* values. (C) Kaplan-Meier analysis of survival length in patient cohorts divided according to low (below the median, $n = 22$, black) and high (above the median, $n = 22$, red) relative expression of *IL1B* mRNA in the blood, as measured by RT-PCR. (D) Kaplan-Meier analysis of survival length in patient cohorts divided according to the relative intestinal expression of *IL1B* (below the median, $n = 22$, black; above the median, $n = 23$, yellow). (E) Relative expression of *IL1B* in the blood in relation to its expression in the intestine in concurrent patient samples ($n = 44$). Linear regression is shown as a continuous red line. (F) Expression of *IL1B* in the blood (red, left, $n = 44$) and in the intestine (yellow, right, $n = 45$). The dashed black lines represent the limits of detection. The p values were corrected for multiple testing when appropriate. Horizontal lines represent the mean \pm SEM; each symbol indicates one sample from one patient.

mRNA between groups in patients with a detectable viral load (22 from 45 patients; $p = 0.83$) (Fig. 2A). We then hypothesized whether SARS-CoV-2 mRNA viremia correlated with survival in our cohort. The viremic and nonviremic groups did not differ significantly in sex, age at death, PMI, or hospitalization rate and only had a significantly different percentage of overweight patients, indicated by their BMI (Fig. 2B). Nonetheless, detectable mRNA for SARS-CoV-2 in the blood was not associated with our cohort's length of survival ($p = 0.38$) (Fig. 2C). So, taken together, *IL1B* levels in the blood are not

associated with the systemic viral load of SARS-CoV-2, nor is the detectability of SARS-CoV-2 in the blood an influencing factor for survival length in the given cohort.

Because IL-1 β has been linked to regulating the production of TGF- β (60), a cytokine that itself is associated with unfavorable outcomes during SARS-CoV-2 infection (61, 62), we hypothesized whether IL-1 β expression might be associated with TGF- β production. Indeed, the patient cohort with elevated levels of *IL1B* showed equally increased levels of systemic *TGFB* ($p = 0.03$) (Fig. 2D, 2E) compared with the *IL1B_{low}* group, whereas other cytokines were not significantly elevated in the systemic *IL1B^{high}* group (Supplemental Fig. 1). On a side note, patients in the systemic *IL1B^{high}* group tended to have elevated (but not statistically significant) lactate levels (Fig. 2F), a standard laboratory marker for sepsis and hemolysis. Beyond this, there was no statistically significant difference between the groups regarding laboratory markers such as liver enzymes, hemoglobin, or thrombocytes (Supplemental Fig. 2). In summary, high levels of *IL1B* in the blood were linked not only to decreased survival time but also to increased *TGFB* expression in the blood. However, no direct connection of systemic IL-1 β to the SARS-CoV-2 viral load in the blood was found.

Table II. Sociodemographic characteristics of COVID-19 deaths ($n = 45$) included in the study

Variable	Median (IQR)/No. (%)
Age, y	79 (71–85)
Sex	
Female	16 (35.6%)
Male	29 (64.4%)
BMI, kg/m ²	26.1 (23.9–31.6)
Hospitalization	33 (73.3%)
Postmortem interval, d	3.0 (2.0–4.0)

IQR, interquartile range.

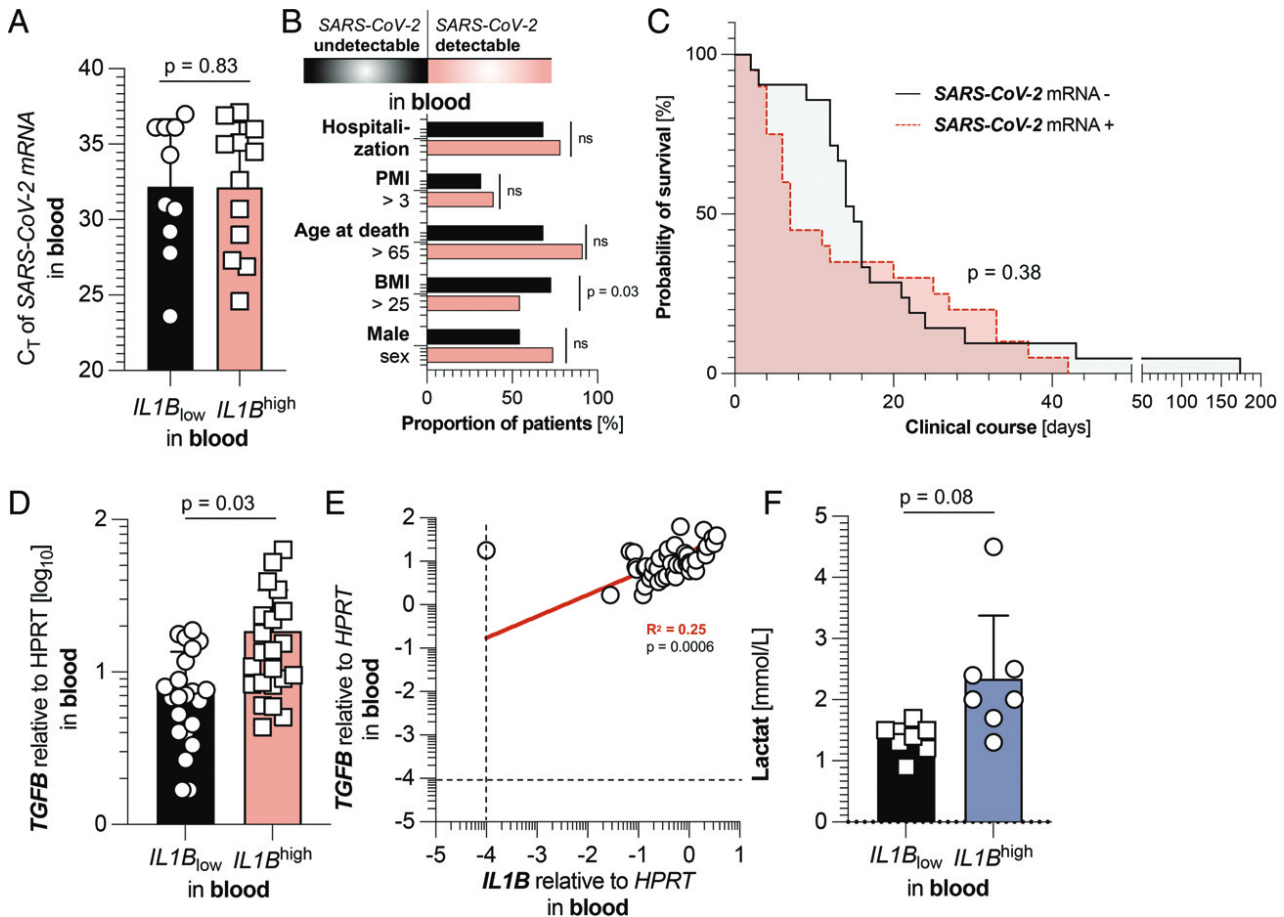


FIGURE 2. Systemic $IL1B$ is not associated with the systemic viral load but correlates with an enhanced $TGFB$ response. **(A)** C_T values of SARS-CoV-2 mRNA expression in the blood of patients with a detectable SARS-CoV-2 viral load ($n = 22$), divided according to low (below the median of all 44 patients, black, $n = 10$) and high (above the median of all 44 patients, red, $n = 12$) expression of $IL1B$. **(B)** Cohort characteristics of patients with undetectable ($n = 23$, black) and detectable ($n = 22$, red) SARS-CoV-2 viral loads. **(C)** Kaplan-Meier analysis of survival length in patient cohorts divided according to undetectability ($n = 23$, black) and detectability ($n = 22$, red) of SARS-CoV-2 mRNA in the blood. **(D)** Relative expression of $TGFB$ in the blood of patients divided according to low (below the median, $n = 22$, black) and high (above the median, $n = 22$, red) relative expression of $IL1B$ mRNA in the blood. **(E)** Relative expression of $IL1B$ in the blood in relation to relative $TGFB$ expression in the blood in concurrent patient samples ($n = 44$). Linear regression is shown as a continuous red line. The dashed black lines represent the limits of detection. **(F)** First available lactate levels (in mmol/L, $n = 14$) upon SARS-CoV-2 diagnosis, determined by screening of patient laboratory findings, divided according to low (below the median of all 44 patients, black, $n = 7$) and high (above the median of all 44 patients, blue, $n = 7$) expression of $IL1B$. The p values were corrected for multiple testing when appropriate. Horizontal lines represent the mean \pm SEM; each symbol indicates one sample from one patient.

Upon SARS-CoV-2 infection, $IL-1\beta$ can be produced by epithelial cells and macrophages in the intestine

Next, we wanted to determine the source of $IL-1\beta$ during SARS-CoV-2 infection in the duodenum by staining the intestinal tissue of six selected deceased individuals for $IL-1\beta$, of which three did not have measurable levels of $IL1B$ RNA (termed $IL1B$ negative) and three had high levels of intestinal $IL1B$ RNA (termed $IL1B$ positive). Indeed, we could detect a small cluster of $IL-1\beta$ -positive cells in $IL1B^{high}$ tissue samples that were absent in $IL1B_{low}$ samples (Fig. 3A). Double-fluorescence staining with IBA1, a commonly used macrophage marker, determined macrophages as one potential source of $IL-1\beta$ in the intestinal epithelium during SARS-CoV-2 infection (Fig. 3B).

Because the count of intestinal epithelial cells is commonly highly reduced in autopsy tissue, and because these cells are often no longer functional, we also analyzed fresh duodenal samples from three patients with SARS-CoV-2 and three control subjects who underwent abdominal surgery with duodenal resection. In these samples, we identified intestinal epithelial cells to be an additional subset of $IL-1\beta$ -producing cells in one patient with proven SARS-CoV-2 infection, but not in the uninfected specimen (Fig. 3C).

To confirm this finding, we generated fresh human intestinal organoids from fresh surgical samples to evaluate the epithelial contribution to $IL-1\beta$ production. Human intestinal organoids already produced $IL-1\beta$ without stimulation (Fig. 3D). We furthermore observed a slight upregulation of $IL-1\beta$ production upon LPS or flagellin stimulation, which was significantly increased by costimulation with SARS-CoV-2 S-protein (Fig. 3D). In summary, both macrophages and intestinal epithelial cells can contribute to intestinal $IL-1\beta$ production responding to SARS-CoV-2 infection.

High levels of $IL1B$ in the intestine are associated with a reduced viral load among individuals with detectable SARS-CoV-2 infection of the intestine

We then assessed the functional contribution of $IL-1\beta$ during the intestinal infection and referred back to the intestinal autopsy tissue of the SARS-CoV-2-positive bodies. Interestingly, when comparing the C_T levels of SARS-CoV-2 mRNA in individuals with a detectable viral load (22 from 45 patients), a significantly increased average C_T value (and thus a decreased viral load) was determined in patients with high intestinal $IL1B$ expression ($p = 0.049$) (Fig. 4A). This observed effect was limited to the small intestine because C_T levels of systemic SARS-CoV-2 mRNA did not differ significantly, nor were

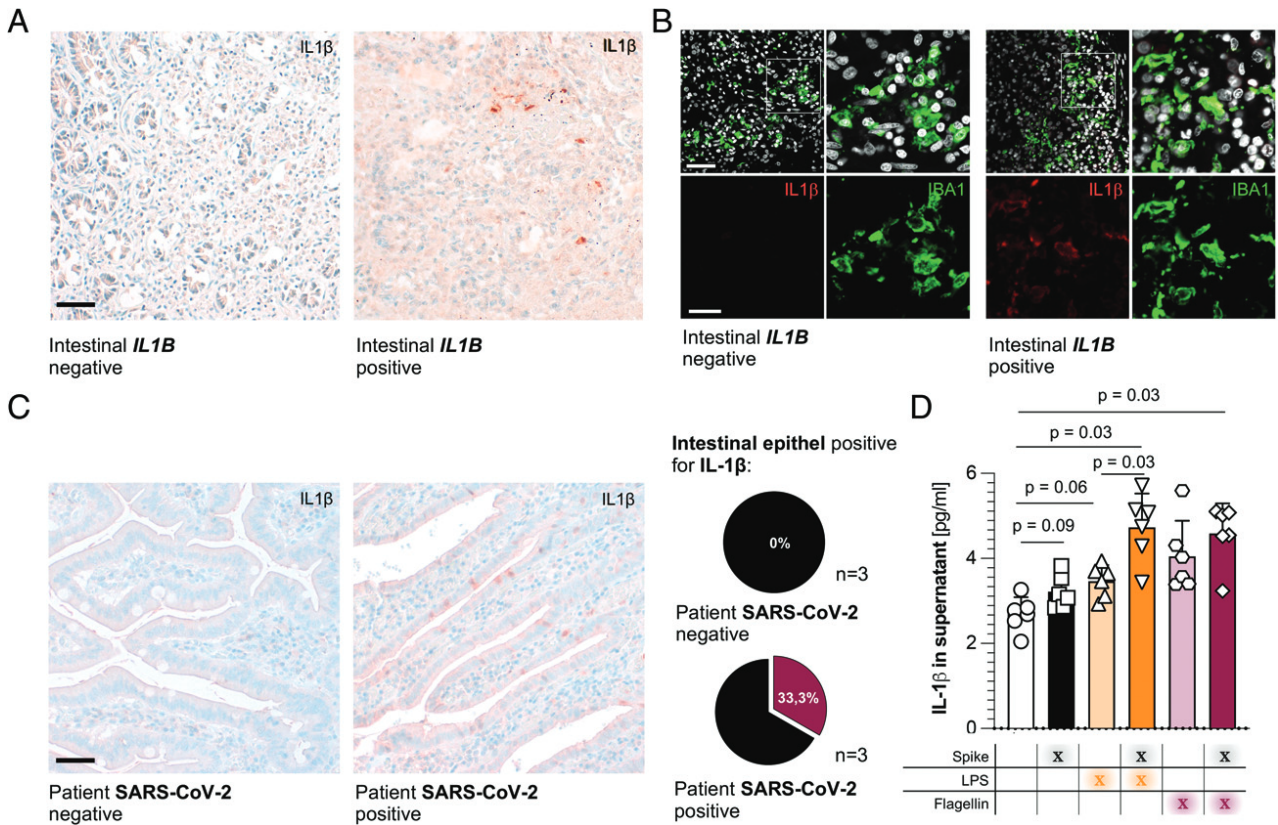


FIGURE 3. IL-1 β can be produced by epithelial cells and macrophages in the intestine during SARS-CoV-2 infection. **(A)** Representative picture of IL-1 β expression, determined by immunohistochemistry, in the duodenum of patients with nondetectable intestinal *IL1B* levels (left) and detectable intestinal *IL1B* levels (right). Tissue samples were taken during the autopsy. Counterstaining and bluing were performed with hematoxylin and Bluing Reagent. Scale bar, 50 μ m. **(B)** Representative picture of IL-1 β (red) and IBA1 (green) expression, determined using double fluorescence, in the duodenum of patients with nondetectable intestinal *IL1B* levels (left four pictures) and detectable intestinal *IL1B* levels (right four pictures). The upper panel represents merged pictures; the lower panel represents unmerged channels. Tissue samples were taken during autopsies. Scale bar, 50 μ m; closeup, 20 μ m. **(C)** Left: Representative picture of IL-1 β expression, determined by immunohistochemistry, in the duodenum of patients without SARS-CoV-2 diagnosis (far left, $n = 3$) and with clinical SARS-CoV-2 diagnosis (middle, $n = 3$). Tissue samples were taken during surgery. Counterstaining and bluing were performed with hematoxylin and Bluing Reagent. Scale bar, 50 μ m. Right: Percentage of patients with detectable IL-1 β expression in the intestinal epithelium. **(D)** IL-1 β expression of human intestinal organoids ($n = 6$), measured in supernatants by ELISA. Suspension organoids were prepared and placed in a differentiation medium for 6 d. Organoids were then stimulated with SARS-CoV-2 S-protein (Spike) (1 μ g/ml), LPS (100 ng/ml), and/or flagellin (100 ng/ml) for 10 h. Data are represented as six biological replicates. Horizontal lines represent the mean \pm SEM; each symbol indicates one biological replicate from a different patient.

they correlated between the intestinal *IL1B^{high}* and *IL1B^{low}* groups ($p = 0.76$) (Fig. 4B). It is well established that detecting SARS-CoV-2 mRNA in multiple organs is associated with decreased

survival time (45, 63); yet, this has not been investigated systematically in the small intestine so far, to our knowledge. When dividing our cohort according to the detectability of

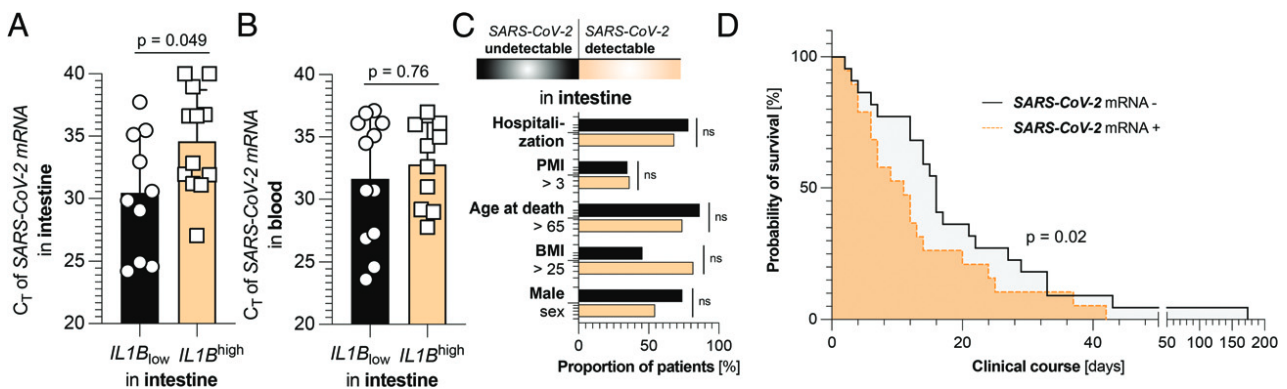


FIGURE 4. High levels of IL-1B in the intestine are associated with a reduced viral load among individuals with detectable SARS-CoV-2 infection of the intestine. **(A)** C_T values of SARS-CoV-2 mRNA expression in the intestines of patients with a detectable SARS-CoV-2 viral load ($n = 22$), divided according to low (below the median of all 44 patients, black, $n = 10$) and high (above the median of all 44 patients, yellow, $n = 12$) expression of intestinal *IL1B*. **(B)** C_T values of SARS-CoV-2 mRNA expression in the blood of patients with a detectable SARS-CoV-2 viral load ($n = 22$), divided according to low (below the median of all 44 patients, black, $n = 12$) and high (above the median of all 44 patients, yellow, $n = 10$) expression of intestinal *IL1B*. **(C)** Cohort characteristics of patients with undetectable ($n = 23$, black) and detectable ($n = 22$, yellow) intestinal SARS-CoV-2 viral loads. **(D)** Kaplan-Meier analysis of survival length in patient cohorts divided according to the absence ($n = 23$, black) or detectability ($n = 22$, yellow) of SARS-CoV-2 mRNA in the intestine. The p values were corrected for multiple testing when appropriate. Horizontal lines represent the mean \pm SEM; each symbol indicates one sample from one patient.

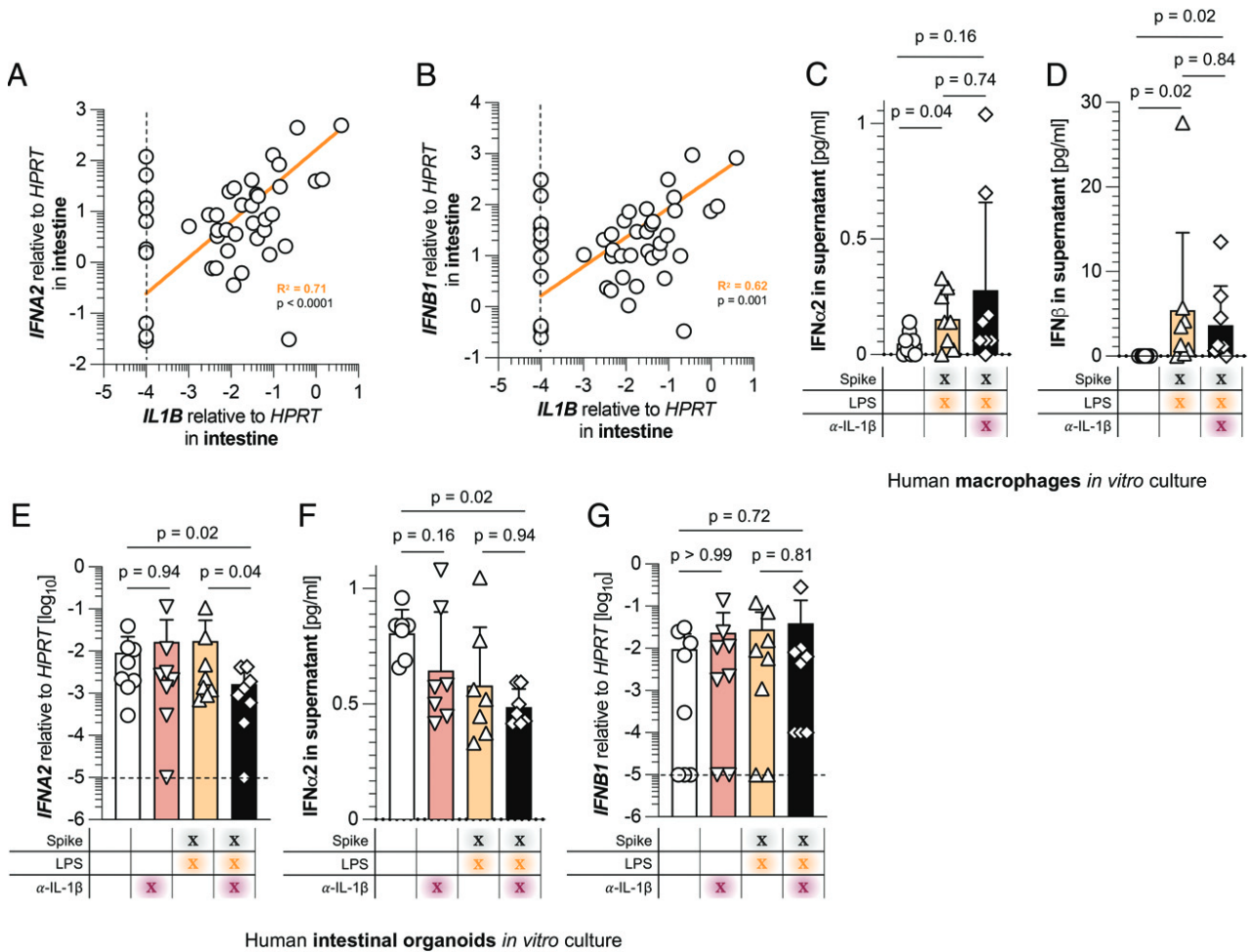


FIGURE 5. IL-1 β sustains RNA expression of *IFN α 2* in intestinal epithelial cells. Relative expression of *IL1B* in the intestine in relation to relative (A) *IFNA2* and (B) *IFNB1* expression in the intestine in concurrent patient samples ($n = 45$). Linear regression is shown as the continuous yellow line. The dashed black lines represent the limits of detection. A pairwise correlation was performed, and p values were Bonferroni corrected for multiple testing. (C) Supernatant protein levels of IFN- α 2 ($n = 8$) and (D) IFN- β ($n = 8$) of *in vitro* expanded human macrophages. Macrophages were stimulated with SARS-CoV-2 S-protein (Spike) (1 μ g/ml), LPS (100 ng/ml), and/or α -IL-1 β (10 μ g/ml) for 24 h. Data are represented as eight biological replicates. (E) Relative expression of *IFNA2* ($n = 8$), (F) supernatant protein levels of IFN- α 2 ($n = 7$), and (G) relative expression of *IFNB1* ($n = 8$) of human intestinal organoids. Suspension organoids were prepared and placed in a differentiation medium for 6 d. Organoids were then stimulated with SARS-CoV-2 S-protein (Spike) (1 μ g/ml), LPS (100 ng/ml), and/or α -IL-1 β (10 μ g/ml) for 24 h (E and G) or 10 h (F). Data are represented as seven or eight biological replicates. Horizontal lines represent the mean \pm SEM; each symbol indicates one sample from one patient.

SARS-CoV-2 mRNA in the intestine, no significant differences regarding sex, BMI, age, PMI, and hospitalization could be discerned (Fig. 4C). However, patients with detectable intestinal SARS-CoV-2 mRNA presented with a significantly decreased survival period ($p = 0.02$) (Fig. 4D). Taken together, intestinal levels of SARS-CoV-2 mRNA are decreased in individuals with detectable local viral load and high intestinal *IL1B* expression. Moreover, the detectability of intestinal SARS-CoV-2 mRNA is associated with a reduced survival period.

IL-1 β sustains RNA expression of IFN α 2 in intestinal epithelial cells

Because local viral loads were reduced in the intestinal *IL1B*^{high} group, we hypothesized that IL-1 β might induce a local antiviral immune response. Among the most upregulated antiviral cytokines are type I IFNs such as IFN α 2 and IFN β 1, with distinct effects against SARS-CoV-2 infection (38–41). Indeed, expression of *IL1B* in the intestines of COVID-19 deceased individuals highly correlated with *IFNA2* ($R^2 = 0.71$; $p < 0.0001$) (Fig. 5A) and *IFNB1* ($R^2 = 0.62$; $p = 0.001$) (Fig. 5B). Interestingly, these correlations between type I IFNs and *IL1B* are indeed intestine-specific, because

levels of *IFNA2* and *IFNB1* did not significantly differ in the systemic *IL1B* groups (Supplemental Fig. 1). Of note, intestinal *IL1B* also correlated with *TNFA* ($R^2 = 0.69$; $p < 0.0001$) (Supplemental Fig. 3K) and with *IL23* ($R^2 = 0.91$; $p < 0.0001$) (Supplemental Fig. 3L), a cytokine that is involved in Th17 cell maturation (64). Apart from these observations, correlations of intestinal *IL1B* with genes connected to other T cell subsets and functions were not found (Supplemental Fig. 3). Explicitly, a correlation between intestinal *IL1B* and intestinal *TGFB*, as it was found for their systemic counterparts, could not be detected in the duodenum.

We next compared the systemic cytokine expression of the intestinal *IL1B*^{high} and *IL1B*^{low} groups. Interestingly, all investigated systemic cytokines were not affected by intestinal IL-1 β expression (Supplemental Fig. 4). Likewise, no significant differences could be detected at all when comparing laboratory findings from patients of the intestinal *IL1B*^{high} and *IL1B*^{low} groups upon diagnosis of SARS-CoV-2 infection (Supplemental Fig. 4).

Finally, we sought to investigate a mechanistic link between intestinal IL-1 β production and upregulation of type I IFNs such as IFN- α 2 and IFN- β 1. Because macrophages were a

significant source of intestinal IL-1 β , we wondered whether this cytokine might induce type I IFNs in macrophages. Thus, we differentiated human macrophages for 1 wk in the presence of M-CSF and then stimulated them with LPS and SARS-CoV-2 S-protein in the presence or absence of an Ab blocking IL-1 β . Although LPS and SARS-CoV-2 S-protein stimulation significantly upregulated IFN- α 2 and IFN- β 1 production from in vitro differentiated macrophages, blockade of IL-1 β did not significantly reduce their expression levels (Fig. 5C, 5D). Thus, macrophage-derived type I IFNs are likely not regulated by IL-1 β .

Next, we wondered whether production of type I IFNs by intestinal epithelial cells is dependent on IL-1 β . Therefore, we treated human intestinal organoids that were stimulated with LPS and SARS-CoV-2 S-protein with an Ab blocking IL-1 β . Indeed, intestinal organoids treated with this IL-1 β blocking Ab showed a decrease in *IFN α 2* RNA expression, but only if stimulated with LPS and S-protein (Fig. 5E). However, this finding could not be confirmed when measuring IFN- α 2 protein concentration in the supernatant of intestinal organoids (Fig. 5F). Because protein concentrations of supernatants are the sum of secreted proteins during an extended time span, whereas RNA expression delivers more acute information, this finding calls for more precise temporal investigations of type I IFNs in the future.

Interestingly, *IFN β 1* expression remained unchanged by IL-1 β blockade (Fig. 5G) and could not be detected as a protein in the supernatant of intestinal organoids (data not shown).

Taken together, IL-1 β sustains intestinal epithelial RNA expression of *IFN α 2* during epithelial cell-derived organoid stimulation with S-protein in vitro, which correlates with protection against SARS-CoV-2 infection-mediated mortality in vivo (Table I).

Discussion

The intestinal tract plays a vital role as a security barrier that, on the one hand, protects against pathogens and, on the other hand, allows the development of tolerance against commensal bacteria and food Ags (5). It is well established that SARS-CoV-2 can also infect the intestinal tract (50, 51). Although systemic and pulmonary immunological responses to SARS-CoV-2 have been thoroughly investigated during the last 2 y, investigations regarding intestinal SARS-CoV-2 infections remain scarce.

In this study, we demonstrated, for the first time, to our knowledge, that detecting SARS-CoV-2 mRNA in the intestine is associated with a decreased time of survival, an observation that has also been established for many other organs (45, 63). Nonetheless, this (to our knowledge) newly found association between SARS-CoV-2 intestinal infection and survival time is somewhat surprising because another study found that involvement of the gastrointestinal tract was linked to a more favorable outcome (52). However, this report used gastrointestinal symptoms such as emesis or diarrhea as the main surrogate marker and not the detectability of SARS-CoV-2 mRNA, which might explain the seemingly opposing findings.

We previously reported that high *TNFA* expression levels in the livers of SARS-CoV-2 deceased individuals correlate with a reduced survival time (54). In contrast, we focused in the present study on the role of intestinal *IL1B*. Taken together, our data showed that elevated expression of intestinal *IL1B* is associated with prolonged survival after infection. However, our study also found that high levels of *IL1B* in the blood were inversely associated with overall survival time. This finding is in line with a previous report revealing a reduced (although not significant) probability of survival in patients with high levels of IL-1 β in the blood (25). Accordingly, systemic blocking of IL-1R, the receptor of IL-1 β , proved beneficial for severe COVID-19 in a recent clinical study (57). Taken together, these former findings

and our data point toward the ambiguous roles of IL-1 β in both the intestine and the blood during COVID-19 infection. Furthermore, blocking of IL-1R also leads to an attenuation of IL-1 α signaling, which might mediate the clinical benefit of anakinra.

We found a strong correlation between *IL1B* and *TGFB* expression in the blood. It is well established that IL-1 β can induce TGF- β production in certain settings (60). Likewise, multiple reports hint at a pathogenic role of TGF- β during COVID-19 infection, such as by reducing protective functions of NK cells (62) or maintaining a chronic and undirected immune response in B lymphocytes (61). Thus, it seems possible that the potential pathogenic role of high *IL1B* in the blood that we found during COVID-19 infection might lie within an induction of TGF- β production. However, further studies are warranted to address this specific point.

We next demonstrated that macrophages were one potential source of IL-1 β in the SARS-CoV-2-infected intestine. However, also other cells, such as intestinal epithelial cells, can produce IL-1 β . Indeed, stimulating the signaling pathways by SARS-CoV-2 S-protein in intestinal epithelial organoids also led to a significant upregulation of IL-1 β production. This finding is in line with a previous study in which S-protein alone was able to bind to TLR4 and activate the TLR4 pathway, which consequently leads to IL-1 β production of the stimulated cell (65). Previous reports furthermore unanimously describe that SARS-CoV-2 mRNA can be detected in intestinal biopsies of patients with COVID-19 (52) and that the virus can infect intestinal organoids (50, 51). Although the effect of SARS-CoV-2 on intestinal IL-1 β production was only marginally investigated before, multiple reports found that SARS-CoV-2 infection leads to an upregulation of IL-1 β production in the lung (29–32).

Finally, we sought to investigate mechanisms underlying the beneficial effects of intestinal IL-1 β and found a strong correlation between *IL1B* on the one hand and type I IFNs on the other hand. Although IL-1 β and type I IFNs are commonly thought to be counterregulated (66–68), both cytokines may also work in an agonistic way under certain conditions (67, 69). Therefore, we used an in vitro intestinal epithelial cell-derived organoid assay and found that S-protein and LPS stimulation alone does not change *IFNA2* expression. However, blockade of IL-1 β under S-protein and LPS stimulation leads to a downregulation of the *IFNA2* transcript. One possible explanation would be that S-protein and LPS stimulation induce several factors, which may induce or suppress *IFNA2* expression. Thus, the overall amount of *IFNA2* does not change. However, further studies will be essential to test this hypothesis. Regardless of this, it is clear that the blockade of IL-1 β does reduce *IFNA2* expression in the presence of S-protein and LPS stimulation, suggesting that, in this setting, the factors suppressing *IFNA2* expression outweigh the factors inducing it. Thus, IL-1 β does impact *IFNA2* expression. However, we cannot exclude the possibility that the presence of the virus in vivo also directly modulates *IFNA2* expression independently of IL-1 β . Moreover, using these in vitro assays, we found that IL-1 β blockade reduced RNA transcripts of *IFN α 2*, but not its overall protein secretion, in the supernatant of this culture. Thus, further studies investigating potential underlying mechanisms of the IL-1 β -dependent post-translational regulation of IFN- α 2 and IFN- β 1 will be critical to further clarify this point.

We furthermore demonstrated a positive correlation between intestinal IL-1 β and IL-23. This finding aligns with current and past literature describing an enhancing role of these cytokines in Th17 differentiation (70). However, the role of intestinal Th17 cells during COVID-19 infections requires further investigation.

Despite all the strengths outlined above, our study possesses some limitations that are important to mention. First, patients were stratified on the basis of *IL1B* RNA expression in either blood or duodenum at the time of their death. Thus, previous dynamics of their *IL1B* expression are totally unknown and could not be used for stratifying these patients. Second, because the production and release of many cytokines, such as IL-1 β and TGF- β , is a multistep process with heavy

post-translational modification involved, the RNA transcripts might only loosely correlate to their biological activity. Third, the stimulation with S-protein is not a full substitute for SARS-CoV-2 infection, which is a further limitation of our study.

Taken together, our data suggest a previously unknown intestinal circuit by which local IL-1 β might enhance and sustain protective responses against SARS-CoV-2, leading to reduced viral loads and thus increased survival time. However, further studies will be important to test this hypothesis. Mechanistically, intestinal IL-1 β sustains RNA expression of IFN- α 2 during intestinal epithelial cell-derived organoid stimulation with S-protein. Our study furthermore supports previous reports indicating a detrimental role of systemic IL-1 β . Thus, these data highlight the opposing roles of intestinal versus systemic IL-1 β and might pave the way for tissue-specific therapies against SARS-CoV-2 infection.

Acknowledgments

We thank Sandra Wende, Cathleen Haueis, and Kristin Hartmann for their excellent technical assistance. We thank the UMIF at UKE for the use of the SP5 microscope. Graphical figures (Fig. 1A and the graphical abstract) were created with BioRender.com. This publication contains data from Nicholas Meins's and Josa Schnell's unpublished medical thesis.

Disclosures

The authors have no financial conflicts of interest.

References

- Bäckhed, F., R. E. Ley, J. L. Sonnenburg, D. A. Peterson, and J. I. Gordon. 2005. Host-bacterial mutualism in the human intestine. *Science* 307: 1915–1920.
- Gill, S. R., M. Pop, R. T. Deboy, P. B. Eckburg, P. J. Turnbaugh, B. S. Samuel, J. I. Gordon, D. A. Relman, C. M. Fraser-Liggett, and K. E. Nelson. 2006. Metagenomic analysis of the human distal gut microbiome. *Science* 312: 1355–1359.
- Iacob, S., D. G. Iacob, and L. M. Luminos. 2019. Intestinal microbiota as a host defense mechanism to infectious threats. *Front. Microbiol.* 9: 3328.
- Oliphant, K., and E. Allen-Vercoe. 2019. Macronutrient metabolism by the human gut microbiome: major fermentation by-products and their impact on host health. *Microbiome* 7: 91.
- Harrison, O. J., and F. M. Powrie. 2013. Regulatory T cells and immune tolerance in the intestine. *Cold Spring Harb. Perspect. Biol.* 5: a018341.
- Lei, Y. M., L. Nair, and M. L. Alegre. 2015. The interplay between the intestinal microbiota and the immune system. *Clin. Res. Hepatol. Gastroenterol.* 39: 9–19.
- McEntee, C. P., C. M. Finlay, and E. C. Lavelle. 2019. Divergent roles for the IL-1 family in gastrointestinal homeostasis and inflammation. *Front. Immunol.* 10: 1266.
- Garlanda, C., C. A. Dinarello, and A. Mantovani. 2013. The interleukin-1 family: back to the future. *Immunity* 39: 1003–1018.
- Takács, L., E. J. Kovacs, M. R. Smith, H. A. Young, and S. K. Durum. 1988. Detection of IL-1 alpha and IL-1 beta gene expression by in situ hybridization. Tissue localization of IL-1 mRNA in the normal C57BL/6 mouse. *J. Immunol.* 141: 3081–3095.
- McLoed, A. G., T. P. Sherrill, D. S. Cheng, W. Han, J. A. Saxon, L. A. Gleaves, P. Wu, V. V. Polosukhin, M. Karin, F. E. Yull, et al. 2016. Neutrophil-derived IL-1 β impairs the efficacy of NF- κ B inhibitors against lung cancer. *Cell Rep.* 16: 120–132.
- Yi, G., M. Liang, M. Li, X. Fang, J. Liu, Y. Lai, J. Chen, W. Yao, X. Feng, L. Hu, et al. 2018. A large lung gene expression study identifying IL1B as a novel player in airway inflammation in COPD airway epithelial cells. *Inflamm. Res.* 67: 539–551.
- Kelly, P., K. G. Meade, and C. O'Farrelly. 2019. Non-canonical inflammasome-mediated IL-1 β production by primary endometrial epithelial and stromal fibroblast cells is NLRP3 and caspase-4 dependent. *Front. Immunol.* 10: 102.
- Sims, J. E., C. J. March, D. Cosman, M. B. Widmer, H. R. MacDonald, C. J. McMahan, C. E. Grubin, J. M. Wignall, J. L. Jackson, S. M. Call, et al. 1988. cDNA expression cloning of the IL-1 receptor, a member of the immunoglobulin superfamily. *Science* 241: 585–589.
- Deyerle, K. L., J. E. Sims, S. K. Dower, and M. A. Bothwell. 1992. Pattern of IL-1 receptor gene expression suggests role in noninflammatory processes. *J. Immunol.* 149: 1657–1665.
- van der Meer, J. W., M. Barza, S. M. Wolff, and C. A. Dinarello. 1988. A low dose of recombinant interleukin 1 protects granulocytopenic mice from lethal gram-negative infection. *Proc. Natl. Acad. Sci. USA* 85: 1620–1623.
- Acosta-Rodriguez, E. V., G. Napolitani, A. Lanzavecchia, and F. Sallusto. 2007. Interleukins 1beta and 6 but not transforming growth factor-beta are essential for the differentiation of interleukin 17-producing human T helper cells. *Nat. Immunol.* 8: 942–949.
- Sutton, C. E., S. J. Lalor, C. M. Sweeney, C. F. Brereton, E. C. Lavelle, and K. H. Mills. 2009. Interleukin-1 and IL-23 induce innate IL-17 production from gamma/delta T cells, amplifying Th17 responses and autoimmunity. *Immunity* 31: 331–341.
- Kiss, M., L. Vande Walle, P. H. V. Saavedra, E. Lebegge, H. Van Damme, A. Murgaski, J. Qian, M. Ehling, S. Pretto, E. Bolli, et al. 2021. IL1 β promotes immune suppression in the tumor microenvironment independent of the inflammasome and gasdermin D. *Cancer Immunol. Res.* 9: 309–323.
- Kersten, K., S. B. Coffelt, M. Hoogstraat, N. J. M. Versteegen, K. Vrijland, M. Ciampricotti, C. W. Doornebal, C. S. Hau, M. D. Wellenstein, C. Salvagno, et al. 2017. Mammary tumor-derived CCL2 enhances pro-metastatic systemic inflammation through upregulation of IL1 β in tumor-associated macrophages. *Oncotarget* 6: e1334744.
- Coffelt, S. B., K. Kersten, C. W. Doornebal, J. Weiden, K. Vrijland, C. S. Hau, N. J. M. Versteegen, M. Ciampricotti, L. J. A. C. Hawinkels, J. Jonkers, and K. E. de Visser. 2015. IL-17-producing $\gamma\delta$ T cells and neutrophils conspire to promote breast cancer metastasis. *Nature* 522: 345–348.
- Friedrich, M., M. Pohin, M. A. Jackson, I. Korsunsky, S. J. Bullers, K. Rue-Albrecht, Z. Christoforidou, D. Sathanathan, T. Thomas, R. Ravindran, et al.; Roche Fibroblast Network Consortium. 2021. IL-1-driven stromal-neutrophil interactions define a subset of patients with inflammatory bowel disease that does not respond to therapies. *Nat. Med.* 27: 1970–1981.
- Li, X. V., I. Leonardi, G. G. Putzel, A. Semon, W. D. Fiers, T. Kusakabe, W. Y. Lin, I. H. Gao, I. Doron, A. Gutierrez-Guerrero, et al. 2022. Immune regulation by fungal strain diversity in inflammatory bowel disease. [Published erratum appears in 2022 *Nature* 608: E21.] *Nature* 603: 672–678.
- Chiaretti, A., S. Pulitanò, G. Barone, P. Ferrara, V. Romano, D. Capozzi, and R. Riccardi. 2013. IL-1 β and IL-6 upregulation in children with H1N1 influenza virus infection. *Mediators Inflamm.* 2013: 495848.
- Negash, A. A., H. J. Ramos, N. Crochet, D. T. Lau, B. Doehle, N. Papic, D. A. Delker, J. Jo, A. Bertoletti, C. H. Hagedorn, and M. Gale, Jr. 2013. IL-1 β production through the NLRP3 inflammasome by hepatic macrophages links hepatitis C virus infection with liver inflammation and disease. *PLoS Pathog.* 9: e1003330.
- Del Valle, D. M., S. Kim-Schulze, H. H. Huang, N. D. Beckmann, S. Nirenberg, B. Wang, Y. Lavin, T. H. Swartz, D. Madduri, A. Stock, et al. 2020. An inflammatory cytokine signature predicts COVID-19 severity and survival. *Nat. Med.* 26: 1636–1643.
- Huang, C., Y. Wang, X. Li, L. Ren, J. Zhao, Y. Hu, L. Zhang, G. Fan, J. Xu, X. Gu, et al. 2020. Clinical features of patients infected with 2019 novel coronavirus in Wuhan, China. *Lancet* 395: 497–506.
- Laing, A. G., A. Lorenc, I. Del Molino Del Barrio, A. Das, M. Fish, L. Monin, M. Muñoz-Ruiz, D. R. McKenzie, T. S. Hayday, I. Francos-Quijorna, et al. 2020. A dynamic COVID-19 immune signature includes associations with poor prognosis. [Published errata appear in 2020 *Nat. Med.* 26: 1663 and 2020 *Nat. Med.* 26: 1951.] *Nat. Med.* 26: 1623–1635.
- Lucas, C., P. Wong, J. Klein, T. B. R. Castro, J. Silva, M. Sundaram, M. K. Ellingson, T. Mao, J. E. Oh, B. Israelow, et al.; Yale IMPACT Team. 2020. Longitudinal analyses reveal immunological misfiring in severe COVID-19. *Nature* 584: 463–469.
- Liao, M., Y. Liu, J. Yuan, Y. Wen, G. Xu, J. Zhao, L. Cheng, J. Li, X. Wang, F. Wang, et al. 2020. Single-cell landscape of bronchoalveolar immune cells in patients with COVID-19. *Nat. Med.* 26: 842–844.
- Xu, G., F. Qi, H. Li, Q. Yang, H. Wang, X. Wang, X. Liu, J. Zhao, X. Liao, Y. Liu, et al. 2020. The differential immune responses to COVID-19 in peripheral and lung revealed by single-cell RNA sequencing. *Cell Discov.* 6: 73.
- Li, S., Y. Zhang, Z. Guan, H. Li, M. Ye, X. Chen, J. Shen, Y. Zhou, Z. L. Shi, P. Zhou, and K. Peng. 2020. SARS-CoV-2 triggers inflammatory responses and cell death through caspase-8 activation. *Signal Transduct. Target. Ther.* 5: 235.
- Zhang, J., H. Wu, X. Yao, D. Zhang, Y. Zhou, B. Fu, W. Wang, H. Li, Z. Wang, Z. Hu, et al. 2021. Pyroptotic macrophages stimulate the SARS-CoV-2-associated cytokine storm. *Cell. Mol. Immunol.* 18: 1305–1307.
- Yan, R., Y. Zhang, Y. Li, L. Xia, Y. Guo, and Q. Zhou. 2020. Structural basis for the recognition of SARS-CoV-2 by full-length human ACE2. *Science* 367: 1444–1448.
- Diamond, M. S., and T. D. Kanneganti. 2022. Innate immunity: the first line of defense against SARS-CoV-2. *Nat. Immunol.* 23: 165–176.
- Wen, W., W. Su, H. Tang, W. Le, X. Zhang, Y. Zheng, X. Liu, L. Xie, J. Li, J. Ye, et al. 2020. Immune cell profiling of COVID-19 patients in the recovery stage by single-cell sequencing. [Published erratum appears in 2020 *Cell Discov.* 6: 41.] *Cell Discov.* 6: 31.
- Ren, X., W. Wen, X. Fan, W. Hou, B. Su, P. Cai, J. Li, Y. Liu, F. Tang, F. Zhang, et al. 2021. COVID-19 immune features revealed by a large-scale single-cell transcriptome atlas. *Cell* 184: 1895–1913.e19.
- Blanco-Melo, D., B. E. Nilsson-Payant, W. C. Liu, S. Uhl, D. Hoagland, R. Möller, T. X. Jordan, K. Oishi, M. Panis, D. Sachs, et al. 2020. Imbalanced host response to SARS-CoV-2 drives development of COVID-19. *Cell* 181: 1036–1045.e9.
- Banerjee, A., N. El-Sayes, P. Budykowski, R. A. Jacob, D. Richard, H. Maan, J. A. Aguiar, W. L. Demian, K. Baid, M. R. D'Agostino, et al. 2021. Experimental and natural evidence of SARS-CoV-2-infection-induced activation of type I interferon responses. *iScience* 24: 102477.
- Onodi, F., L. Bonnet-Madin, L. Meertens, L. Karpf, J. Poirot, S. Y. Zhang, C. Picard, A. Puel, E. Jouanguy, Q. Zhang, et al. 2021. SARS-CoV-2 induces human plasmacytoid dendritic cell diversification via UNC93B and IRAK4. *J. Exp. Med.* 218: e20201387.

40. Rebendenne, A., A. L. C. Valadao, M. Tazuet, G. Maarifi, B. Bonaventure, J. McKellar, R. Planes, S. Nisole, M. Arnaud-Arnould, O. Moncorge, and C. Goujon. 2021. SARS-CoV-2 triggers an MDA-5-dependent interferon response which is unable to control replication in lung epithelial cells. *J. Virol.* 95: e02415-20.
41. Yin, X., L. Riva, Y. Pu, L. Martin-Sancho, J. Kanamune, Y. Yamamoto, K. Sakai, S. Gotoh, L. Miorin, P. D. De Jesus, et al. 2021. MDA5 governs the innate immune response to SARS-CoV-2 in lung epithelial cells. *Cell Rep.* 34: 108628.
42. Bastard, P., Q. Zhang, S. Y. Zhang, E. Jouanguy, and J. L. Casanova. 2022. Type I interferons and SARS-CoV-2: from cells to organisms. *Curr. Opin. Immunol.* 74: 172–182.
43. Zhu, N., D. Zhang, W. Wang, X. Li, B. Yang, J. Song, X. Zhao, B. Huang, W. Shi, R. Lu, et al.; China Novel Coronavirus Investigating and Research Team. 2020. A novel coronavirus from patients with pneumonia in China, 2019. *N. Engl. J. Med.* 382: 727–733.
44. Bräuninger, H., B. Stoffers, A. D. E. Fitzek, K. Meißner, G. Aleshcheva, M. Schweizer, J. Weimann, B. Rotter, S. Warnke, C. Edler, et al. 2022. Cardiac SARS-CoV-2 infection is associated with pro-inflammatory transcriptomic alterations within the heart. *Cardiovasc. Res.* 118: 542–555.
45. Braun, F., M. Lütgehetmann, S. Pfeifferle, M. N. Wong, A. Carsten, M. T. Lindenmeyer, D. Nörz, F. Heinrich, K. Meißner, D. Wichmann, et al. 2020. SARS-CoV-2 renal tropism associates with acute kidney injury. *Lancet* 396: 597–598.
46. Jansen, J., K. C. Reimer, J. S. Nagai, F. S. Varghese, G. J. Overheul, M. de Beer, R. Roverts, D. Daviran, L. A. S. Fermin, B. Willemsen, et al.; COVID Moonshot consortium. 2022. SARS-CoV-2 infects the human kidney and drives fibrosis in kidney organoids. *Cell Stem Cell* 29: 217–231.e8.
47. Puelles, V. G., M. Lütgehetmann, M. T. Lindenmeyer, J. P. Sperhake, M. N. Wong, L. Allweiss, S. Chilla, A. Heinemann, N. Wanner, S. Liu, et al. 2020. Multiorgan and renal tropism of SARS-CoV-2. *N. Engl. J. Med.* 383: 590–592.
48. Wanner, N., G. Andrieux, P. Badia-I-Mompel, C. Edler, S. Pfeifferle, M. T. Lindenmeyer, C. Schmidt-Lauber, J. Czogalla, M. N. Wong, Y. Okabayashi, et al. 2022. Molecular consequences of SARS-CoV-2 liver tropism. *Nat. Metab.* 4: 310–319.
49. Zhang, H., H. B. Li, J. R. Lyu, X. M. Lei, W. Li, G. Wu, J. Lyu, and Z. M. Dai. 2020. Specific ACE2 expression in small intestinal enterocytes may cause gastrointestinal symptoms and injury after 2019-nCoV infection. *Int. J. Infect. Dis.* 96: 19–24.
50. Lamers, M. M., J. Beumer, J. van der Vaart, K. Knoops, J. Puschhof, T. I. Breugem, R. B. G. Ravelli, J. Paul van Schayck, A. Z. Mykytyn, H. Q. Duimel, et al. 2020. SARS-CoV-2 productively infects human gut enterocytes. *Science* 369: 50–54.
51. Zhou, J., C. Li, X. Liu, M. C. Chiu, X. Zhao, D. Wang, Y. Wei, A. Lee, A. J. Zhang, H. Chu, et al. 2020. Infection of bat and human intestinal organoids by SARS-CoV-2. *Nat. Med.* 26: 1077–1083.
52. Livanos, A. E., D. Jha, F. Cossarini, A. S. Gonzalez-Reiche, M. Tokuyama, T. Aydllo, T. L. Parigi, M. S. Ladinsky, I. Ramos, K. Dunleavy, et al. 2021. Intestinal host response to SARS-CoV-2 infection and COVID-19 outcomes in patients with gastrointestinal symptoms. *Gastroenterology* 160: 2435–2450.e34.
53. Song, P., W. Li, J. Xie, Y. Hou, and C. You. 2020. Cytokine storm induced by SARS-CoV-2. *Clin. Chim. Acta* 509: 280–287.
54. Lücke, J., M. Nawrocki, J. Schnell, N. Meins, F. Heinrich, T. Zhang, F. Bertram, M. Sabihi, M. Böttcher, T. Blankenburg, et al. 2023. TNF α aggravates detrimental effects of SARS-CoV-2 infection in the liver. *Front. Immunol.* 14: 1151937.
55. Guimarães, P. O., D. Quirk, R. H. Furtado, L. N. Maia, J. F. Saraiva, M. O. Antunes, R. Kalil Filho, V. M. Junior, A. M. Soeiro, A. P. Tognon, et al.; STOP-COVID Trial Investigators. 2021. Tofacitinib in patients hospitalized with Covid-19 pneumonia. *N. Engl. J. Med.* 385: 406–415.
56. REMAP-CAP Investigators. 2021. Interleukin-6 receptor antagonists in critically ill patients with Covid-19. *N. Engl. J. Med.* 384: 1491–1502.
57. Kyriazopoulou, E., T. Huet, G. Cavalli, A. Gori, M. Kyprianou, P. Pickkers, J. Eugen-Olsen, M. Clerici, F. Veas, G. Chatellier, et al.; International Collaborative Group for Anakinra in COVID-19. 2021. Effect of anakinra on mortality in patients with COVID-19: a systematic review and patient-level meta-analysis. *Lancet Rheumatol.* 3: e690–e697.
58. Edler, C., A. S. Schröder, M. Aepfelbacher, A. Fitzek, A. Heinemann, F. Heinrich, A. Klein, F. Langenwalder, M. Lütgehetmann, K. Meißner, et al. 2020. Dying with SARS-CoV-2 infection—an autopsy study of the first consecutive 80 cases in Hamburg, Germany. [Published erratum appears in 2020 *Int. J. Legal Med.* 134: 1977.] *Int. J. Legal Med.* 134: 1275–1284.
59. Jung, J. M., W. Ching, M. E. Baumdick, H. Hofmann-Sieber, J. B. Bosse, T. Koyro, K. J. Möller, L. Wegner, A. Niehrs, K. Russu, et al. 2021. KIR3DS1 directs NK cell-mediated protection against human adenovirus infections. *Sci. Immunol.* 6: eabe2942.
60. Yue, T. L., X. K. Wang, B. Olson, and G. Feuerstein. 1994. Interleukin-1 beta (IL-1 beta) induces transforming growth factor-beta (TGF-beta 1) production by rat aortic smooth muscle cells. *Biochem. Biophys. Res. Commun.* 204: 1186–1192.
61. Ferreira-Gomes, M., A. Kruglov, P. Durek, F. Heinrich, C. Tizian, G. A. Heinz, A. Pascual-Reguant, W. Du, R. Mothes, C. Fan, et al. 2021. SARS-CoV-2 in severe COVID-19 induces a TGF- β -dominated chronic immune response that does not target itself. *Nat. Commun.* 12: 1961.
62. Witkowski, M., C. Tizian, M. Ferreira-Gomes, D. Niemyer, T. C. Jones, F. Heinrich, S. Frischbutter, S. Angermair, T. Hohnstein, I. Mattioli, et al. 2021. Untimely TGF β responses in COVID-19 limit antiviral functions of NK cells. *Nature* 600: 295–301.
63. Heinrich, F., M. F. Nentwich, E. Bibiza-Freiwald, D. Norz, K. Roedl, M. Christner, A. Hoffmann, F. Olearo, S. Kluge, M. Aepfelbacher, et al. 2021. SARS-CoV-2 blood RNA load predicts outcome in critically ill COVID-19 patients. *Open Forum Infect. Dis.* 8: ofab509.
64. Ghoreschi, K., A. Laurence, X. P. Yang, C. M. Tato, M. J. McGeachy, J. E. Konkel, H. L. Ramos, L. Wei, T. S. Davidson, N. Bouladoux, et al. 2010. Generation of pathogenic T(H)17 cells in the absence of TGF- β signalling. *Nature* 467: 967–971.
65. Zhao, Y., M. Kuang, J. Li, L. Zhu, Z. Jia, X. Guo, Y. Hu, J. Kong, H. Yin, X. Wang, and F. You. 2021. SARS-CoV-2 spike protein interacts with and activates TLR41. [Published erratum appears in 2021 *Cell Res.* 31: 825.] *Cell Res.* 31: 818–820.
66. Castiglia, V., A. Piersigilli, F. Ebner, M. Janos, O. Goldmann, U. Damböck, A. Kröger, S. Weiss, S. Knapp, A. M. Jamieson, et al. 2016. Type I interferon signaling prevents IL-1 β -driven lethal systemic hyperinflammation during invasive bacterial infection of soft tissue. *Cell Host Microbe* 19: 375–387.
67. Labzin, L. I., M. A. Lauterbach, and E. Latz. 2016. Interferons and inflammasomes: cooperation and counterregulation in disease. *J. Allergy Clin. Immunol.* 138: 37–46.
68. Man, S. M., and T. D. Kanneganti. 2016. Type I interferon keeps IL-1 β in check. *Cell Host Microbe* 19: 272–274.
69. Aarberg, L. D., C. Wilkins, H. J. Ramos, R. Green, M. A. Davis, K. Chow, and M. Gale, Jr. 2018. Interleukin-1 β signaling in dendritic cells induces antiviral interferon responses. *MBio* 9: e00342-18.
70. Santarlasci, V., L. Cosmi, L. Maggi, F. Liotta, and F. Annunziato. 2013. IL-1 and T helper immune responses. *Front. Immunol.* 4: 182.